Excited-state Properties of $[(OC)_5W(L)W(CO)_5]$ [L = 4,4'-bipyridyl (4,4'-bipy) or pyrazine] and $[(OC)_5W(4,4'\text{-bipy})]$

Michael W. George,* Frank P. A. Johnson, James J. Turner* and Jeremy R. Westwell
Department of Chemistry, University of Nottingham, University Park, Nottingham NG7 2RD, UK

Fast time-resolved infrared (TRIR) spectroscopy has been employed to probe the electron distribution in the lowest metal-to-ligand charge-transfer excited states of $[(OC)_5W(4,4'\text{-bipy})W(CO)_5]$ **1**, $[(OC)_5W(4,4'\text{-bipy})]$ **2** (4,4'-bipy = 4,4'-bipyridyl) and $[(OC)_5W(pyz)W(CO)_5]$ **3** (pyz = pyrazine). The excited state of **1** (*i.e.* **1***) shows a ν(CO) band pattern, compared with the ground state, in which some ν(CO) bands increase and some decrease in frequency; those which increase match very closely those observed for the excited state of **2**, where the increase in frequency is readily assigned to the increase in the effective oxidation state of W on electron transfer to the 4,4'-bipy ligand (schematically W^+L^-). The ν(CO) IR bands of the electrochemically reduced **1**, *i.e.* $\mathbf{1}^-$, are lower in frequency than those of **1**, and nearly match the low-frequency bands of **1***. The interpretation is that the excited state of **1** is localised (schematically $\approx W^+L^-W$) on the IR time-scale, and that the degree of coupling between the two halves of the excited molecule is very small. Similar conclusions are obtained for the excited state of **3**, based on TRIR and spectroelectrochemistry of this complex.

Complexes of formula $[(OC)_5M(L)M(CO)_5]$, where M = Cr, Mo or W, and L is a bridging ligand containing two nitrogen donors such as pyrazine (pyz) or 4,4'-bipyridyl (4,4'-bipy) have been the subject of much interest,[1-6] partly because of the opportunity to probe the effects on the photophysical and redox properties of changing from the monomer, $[(OC)_5M(L)]$, to the dimer, $[(OC)_5M(L)M(CO)_5]$, but also because the electron-transfer properties of the excited states of the dimers are of fundamental importance.

An excited-state scheme for $[(OC)_5W(4,4'\text{-bipy})W(CO)_5]$ **1**, and $[(OC)_5W(4,4'\text{-bipy})]$ **2**, based on a study by Lees and co-workers[2-4] is shown in Fig. 1. Each complex exhibits a low lying ligand field (LF) and metal-to-ligand charge-transfer (MLCT) state. The LF state is dissociative, involving W–N cleavage, and the MLCT state involves charge transfer from the metal to the π^* orbital of 4,4'-bipy. For both the mono- and di-nuclear complexes, the MLCT transition is the lower in energy. Dimerisation (*i.e.* **2** ⟶ **1**) causes a lowering of the π^* orbital of the 4,4'-bipy ligand, and so the difference in energy between the MLCT and LF states is greater for **1** than for **2**. Previous work[7] had suggested that, for **2** the LF state was at lower energy than the MLCT state. Among other results, the following time-resolved infrared study resolves this difference. For the pyz analogue of the dinuclear complex, $[(OC)_5W(pyz)W(CO)_5]$ **3**, the MLCT again is lower in energy than the LF state, this time with a substantial difference. However for the monomer, $[(OC)_5W(pyz)]$ **4**, the LF is believed to be at lower energy.[2]

Dodsworth and Lever[6] noted that the excited state of **3**, in which there is electron transfer to the bridging pyrazine, formally $[W^+(pyz^-)W^0]$, is related to the ground state of the Creutz–Taube ion, $[(H_3N)_5Ru(pyz)Ru(NH_3)_5]^{5+}$; the former can be written as $[W(d^5)(pyz^-)W(d^6)]$, and the latter as $[Ru(d^5)(pyz)Ru(d^6)]$. A similar analogy exists between **1** and $[(H_3N)_5Ru(4,4'\text{-bipy})Ru(NH_3)_5]^{5+}$. The Creutz–Taube ion is believed to be delocalised, mixed-valence Class III, whereas $[(H_3N)_5Ru(4,4'\text{-bipy})Ru(NH_3)_5]^{5+}$ is Class II, with an estimated $k_{el} > 10^8$ s^{-1}, where k_{el} is the rate constant associated with electron transfer.[8] The whole area of mixed-valence ruthenium complexes has been reviewed recently.[8] Thus, for the metal carbonyl species **1** and **3**, there is an interesting question as to whether the excited states show localised or delocalised behaviour on the IR time-scale. In recent experiments McGarvey and co-workers[9] have shown that in the excited state of **1**, the resonance-Raman spectra confirm that the bridging ligand is best described as (4,4'-bipy)$^-$, but there was no resonance enhancement of ν(CO) vibrations, and thus no definite information as to whether the excited state is localised or delocalised. In the present paper, these questions are probed by fast time-resolved infrared (TRIR) spectroscopy, and by infrared spectroelectrochemistry which demonstrate that both **1** and **3** have *localised* MLCT states. Preliminary results have been communicated.[10] The significance of the ν(CO) shifts from ground to excited states are discussed and interpreted in terms of Class I behaviour,[11] *i.e.* with coupling between the two halves of the molecule approximately equal to zero.

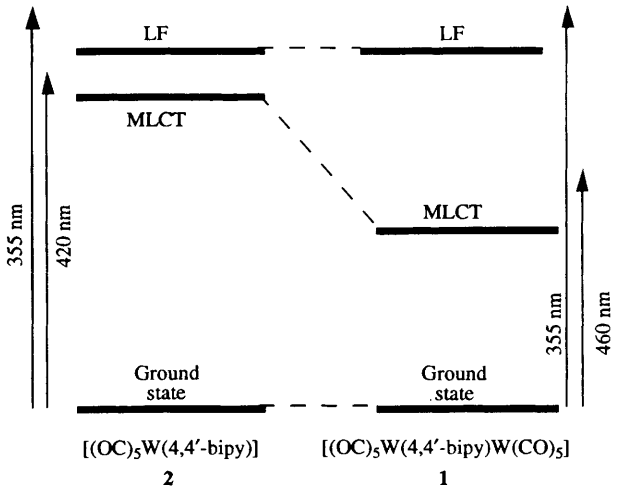

Fig. 1 Schematic diagram of the relative energies of the LF and MLCT states for the complexes $[(OC)_5W(4,4'\text{-bipy})W(CO)_5]$ **1** and $[(OC)_5W(4,4'\text{-bipy})]$ **2** based on previous studies by Lees and co-workers.[2-4] Arrows indicate the various photolysis wavelengths (not to scale) employed in the TRIR experiments described in the text

Table 1 Infrared vibrational data, in the ν(CO) region (in cm^{-1}), for the ground and excited states of $[(OC)_5W(4,4'\text{-bipy})W(CO)_5]$ **1**, $[(OC)_5W(4,4'\text{-bipy})]$ **2** and $[(OC)_5W(pyz)W(CO)_5]$ **3** in CH_2Cl_2 solution

	Ground state		Excited state[a]			
Complex	FTIR[b]	TRIR[c]	(i) TRIR	Δ ν(CO)[d]	(ii) TRIR	Δ ν(CO)[d]
1	2072 (a_1, w)	2073	2105	+33	2059	−13
	1933 (e, vs)	1936	~2010	+77	~1915	−18
	1901 (a_1, m)	1900	~1970	+69	~1875	−26
2	2073 (a_1, w)	2074	2104	+31		
	1930 (e, vs)	1933	2005	+75		
	1901 (a_1, m)	1890	1965	+64		
3	2069 (a_1, w)	2068	2105	+36	2046	−23
	1942 (e, vs)	1942	2003	+61	~1918	−24
	1911 (a_1, m)	?	1978	+65	~1872	−39

[a] The excited-state bands are grouped into: (i) those increasing in frequency, (ii) those decreasing in frequency. [b] FTIR measured in CH_2Cl_2 (5×10^{-4} mol dm^{-3}); very weak shoulders appear at ≈1973 (**1**), ≈1974 (**2**) and ≈1981 (**3**) cm^{-1} due to the b_1 bands, which are formally forbidden under C_{4v} symmetry. [c] The positions of the ground-state bands can also be determined from TRIR, less accurately, from the loss on excitation. [d] The shift is measured from the ground state FTIR to the excited state TRIR.

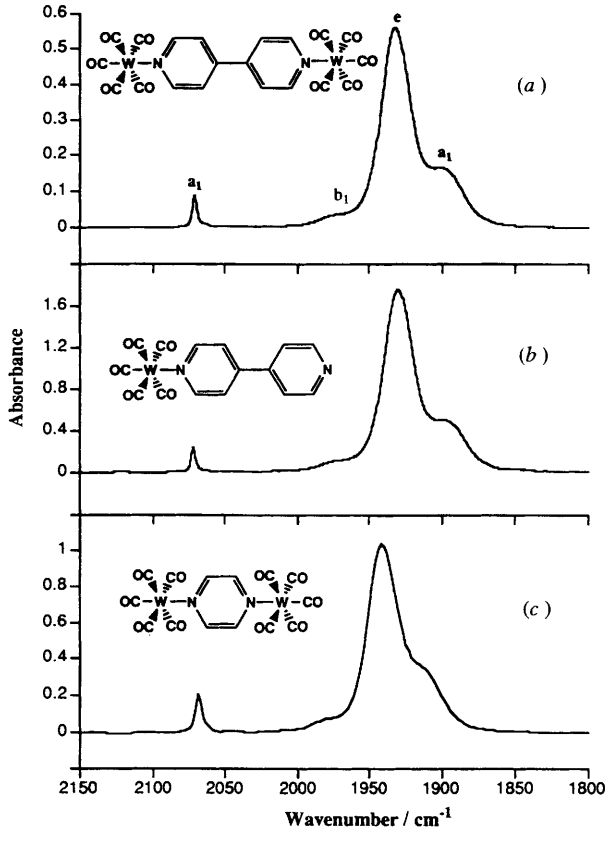

Fig. 2 FTIR spectra in the ν(CO) region (CH_2Cl_2 solution) of (*a*) $[(OC)_5W(4,4'\text{-bipy})W(CO)_5]$ (≈5×10^{-4} mol dm^{-3}, path length 1 mm), (*b*) $[(OC)_5W(4,4'\text{-bipy})]$ (≈2×10^{-3} mol dm^{-3}, 1 mm) and (*c*) $[(OC)_5W(pyz)W(CO)_5]$ (≈5×10^{-4} mol dm^{-3}, 2.5 mm)

Experimental

Samples.—We are very grateful to Dr. P. Mountford for his help and advice with the synthesis of **1** and **2**, which were prepared by slight modification of literature methods.[2,12] Samples of **1** and **3**, and of **2** were also supplied by Professor A. J. Lees and Dr. J. J. McGarvey, respectively. They were used without further purification. Unfortunately **2** readily dimerises to **1** as shown below. This introduces complications into the photochemistry of **2** which can be avoided[12] by adding excess 4,4'-bipy to solutions of **2**; such solutions were used in the experiments described here. Unfortunately the excited state of **4** is too short-lived (≈20 ns) at room temperature for study by our current equipment.

$$2[(OC)_5W(4,4'\text{-bipy})] \rightleftharpoons [(OC)_5W(4,4'\text{-bipy})W(CO)_5] + 4,4'\text{-bipy}$$

Infrared spectra of **1**, **2** and **3** in the ν(CO) region are shown in Fig. 2, and details are given in Table 1. On the basis of local C_{4v} symmetry, the most intense features are readily assigned to the two a_1 and e modes; the weak features are assigned to the b_1 modes, partially allowed because in principle N-donor ligands lower the symmetry.

Time-resolved IR Apparatus.—The Nottingham TRIR apparatus has been described elsewhere.[13] Briefly it consists of a pulsed UV source to initiate photochemical reaction and a continuous-wave IR laser to monitor the transient IR absorptions. The pulsed UV/VIS source was provided by either a Nd/YAG laser operating at 355 or 532 nm, or by an excimer-pumped dye laser emitting at 420 (Stilbene 420), 460 (Coumarin 460) or 510 nm (Coumarin 510). Two different monitoring lasers were used, either an Edinburgh Instruments PL3 CO laser, line tunable in steps of *ca.* 4 cm^{-1} over a limited wavenumber range (≈2000–1550 cm^{-1}), or a Mütek IR diode laser (model MDS 1100, fitted with Mütek MDS 1200) (1700–2200 cm^{-1}). Changes in IR absorption at a particular wavelength were detected by a photovoltaic 77 K HgCdTe detector (Laser Monitoring Systems PV 2180) and IR spectra are built up on a 'point-by-point' basis. The selection of UV or visible wavelength for photoinitiation was influenced by the relative positions of the LF and MLCT absorptions and also by experimental limitations, which precluded the use of our IR diode laser with the dye laser, due to its highly divergent beam. Thus to probe the region above ≈2000 cm^{-1}, where it was necessary to use the diode IR laser, we could only photolyse at 355 nm. Infrared and UV/VIS spectra were recorded on Perkin-Elmer system 2000 Fourier-transform (FT) IR and Perkin-Elmer Lambda 16 instruments respectively. All TRIR experiments were performed in CH_2Cl_2 (Aldrich HPLC grade) which was distilled over CaH_2 before use.

IR Spectroelectrochemistry.—Infrared spectroelectrochemical measurements were made using a continuous-flow column electrolytic method.[14] The working electrode consists of many strands of 0.1 mm Pt wire contained inside a porous Vycor™ glass tube. Argon-purged solutions of **1** or **3** (0.2–0.4 mmol dm^{-3}) in acetonitrile solution containing NBu_4PF_6 as the electrolyte (≈0.1 mol dm^{-3}) were passed through the electrode at ≈0.4–0.5 cm^3 min^{-1}, then, following electrolysis, were passed through an IR flow cell for spectral investigation. Acetonitrile (Aldrich HPLC grade) was dried over CaH_2; NBu_4PF_6 (Aldrich) was dried in an oven before use.

Results and Discussion

TRIR of Excited States of $[(OC)_5W(4,4'\text{-bipy})W(CO)_5]$ **1** *and* $[(OC)_5W(4,4'\text{-bipy})]$ **2**.—In the ν(CO) IR spectra of the excited states of **1** and **2**, there is considerable overlap of bands in the region associated with the e and low-frequency a_1 modes (see later). However, consideration of the high-frequency a_1 bands provides a direct understanding of a considerable part of the excited-state properties. This in turn leads to an understanding of the lower frequency region. The high-frequency region has been described in a preliminary communication[10]; for completeness we repeat some of the points made therein.

The TRIR experiments in this region, using a photolysis wavelength of 355 nm, are summarised in Fig. 3; the band positions are shown in Table 1. In Fig. 3(*a*) it is clear that there is loss of the parent band of **1** at 2073 cm^{-1}, and the generation of two new bands at 2105 and 2059 cm^{-1}. These bands decay with lifetimes of ≈160 and ≈170 ns [Fig. 4(*a*) and Table 2] respectively, and hence, within experimental error, can be assigned to the same MLCT excited species, **1***; emission experiments[12] gave a lifetime of 125 ns. Fig. 3(*b*) shows parent **2** depletion (at 2074 cm^{-1}), and the generation of only one intense new band (at 2104 cm^{-1}) and a small absorption at 2088 cm^{-1}. The band at 2104 cm^{-1} decays with a lifetime of ≈220 ns [Fig. 4(*b*) and Table 2] and is assigned to the MLCT excited state of **2**, *i.e.* **2***; emission experiments[12] gave a lifetime of 260 ns. The shift in frequency of the ν(CO) a_1 band of **2** from the ground to the excited state is consistent with the transfer of charge from W to 4,4'-bipy. [*i.e.* $(OC)_5W^+(4,4'\text{-bipy}^-)$] which results in less backbonding to the CO groups and hence an increase in frequency; an LF state would be expected to give a different shift.[15] The lifetimes of the excited states of **1** and **2** vary from those published previously[4] (394 and 415 ns respectively), measured by emission spectroscopy in benzene, the difference being accounted for by the change in solvent.

The small absorption at 2088 cm^{-1} [Fig. 3(*b*)] is assigned to the high-frequency a_1 mode of solvated $W(CO)_5$ [*i.e.* $(OC)_5W\cdots CH_2Cl_2$] by comparison with previous studies in heptane solution.[16] This is produced 'instantaneously' because of overlap between the excitation source at 355 nm and the LF absorption band of **2** (see Fig. 1) which results in direct ejection of the 4,4'-bipy ligand [equation (1), solv = solvent]. Within

$$[(OC)_5W(4,4'\text{-bipy})] \xrightarrow{h\nu} (OC)_5W + 4,4'\text{-bipy} \xrightarrow{solv} (OC)_5W\cdots solv \quad (1)$$

experimental uncertainty, there is no evidence for this weak band of $(OC)_5W\cdots$solv from photolysis of **1** shown in Fig. 3(*a*), presumably because of the lower quantum yield[3] for equation (2).

$$[(OC)_5W(4,4'\text{-bipy})W(CO)_5] \xrightarrow{h\nu} (OC)_5W + (4,4'\text{-bipy})W(CO)_5 \quad (2)$$

As the lowest excited state of **1** involves electron transfer to the bridging ligand, there are two possible extremes for the charge distribution in the excited state, described as either $(OC)_5W^{(\approx +\frac{1}{2})}(4,4'\text{-bipy})^{(\approx -1)}W^{(\approx +\frac{1}{2})}(CO)_5$ (*i.e.*, delocalised) or $(OC)_5W^{(\approx +1)}(4,4'\text{-bipy})^{(\approx -1)}W^{(\approx 0)}(CO)_5$ (i.e., localised).

If the charge were delocalised, the ν(CO) *pattern* for **1*** would be expected to be similar to that of **2***, that is the production of one new band to higher frequency, relative to the parent but with an observed shift approximately half that observed for **2***, corresponding to the lower formal charge on the metal. This is analogous to the elegant spectroelectrochemical experiments[17] on $[\{(Pr^i_3P)_2(OC)_3Mo\}_2(\mu\text{-pyz})]$ **5**. The ν(CO) spectrum of the cation $\mathbf{5}^+$ shows a pattern consistent with delocalisation, *i.e.*, $Mo^{+\frac{1}{2}}Mo^{+\frac{1}{2}}$; ESR data show that the Mo coupling in $\mathbf{5}^+$ is only about one half that in the monomer cation,

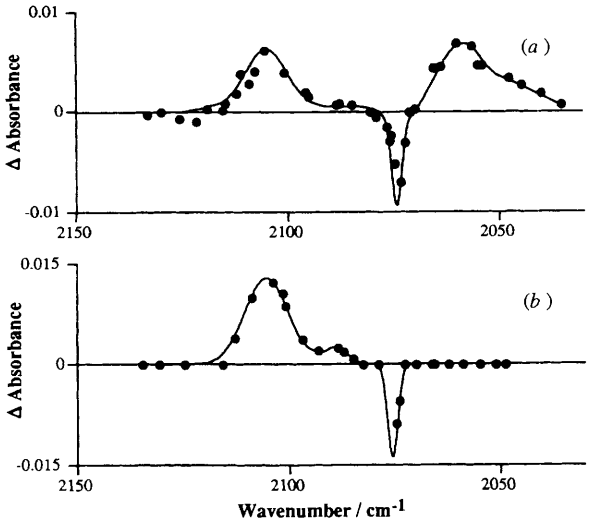

Fig. 3 (*a*) TRIR spectrum at ≈85 ns after flash (355 nm, ≈40 mJ) of $[(OC)_5W(4,4'\text{-bipy})W(CO)_5]$ in CH_2Cl_2 (≈3.5 × 10^{-3} mol dm^{-3}, path length 1 mm); (*b*) TRIR spectrum at ≈65 ns after flash (355 nm, ≈30 mJ) of $[(OC)_5W(4,4'\text{-bipy})]$ plus excess 4,4'-bipy in CH_2Cl_2 (≈2 × 10^{-3} and ≈2 × 10^{-2} mol dm^{-3}, respectively, path length 1 mm). The dots represent the actual laser frequencies and the solid lines simply illustrate the various peaks

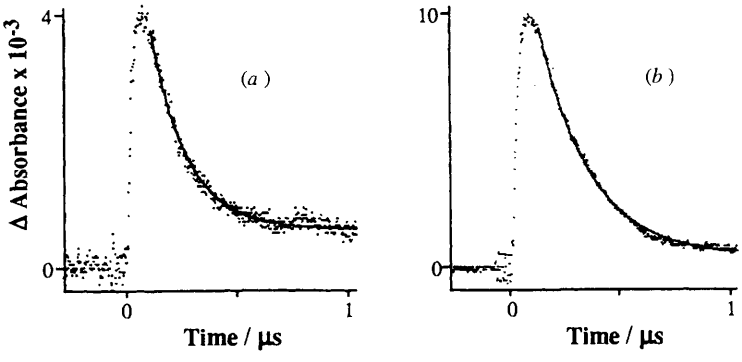

Fig. 4 (*a*) A trace showing the change in intensity of one of the excited-state bands of $[(OC)_5W(4,4'\text{-bipy})W(CO)_5]$, recorded at 2108 cm^{-1}; (*b*) a similar trace for an excited-state band of $[(OC)_5W(4,4'\text{-bipy})]$, recorded at 2108 cm^{-1}. The continuous lines represent exponential fits to the decay data with lifetimes of 160 and 220 ns respectively; the second band of $[(OC)_5W(4,4'\text{-bipy})W(CO)_5]$ (not shown) also decays exponentially with a lifetime of ≈170 ns, thus confirming that the two ν(CO) bands in Fig. 3(*a*) refer to the same excited state. A small residual absorbance is seen in (*a*) due to a small acoustic 'shock' wave which occurs at all frequencies during this experiment

Table 2 Summary of the kinetic measurements[a] made in the TRIR experiments on $[(OC)_5W(4,4'\text{-bipy})W(CO)_5]$ **1**, $[(OC)_5W(4,4'\text{-bipy})]$ **2** and $[(OC)_5W(pyz)W(CO)_5]$ **3** in CH_2Cl_2 solution. All rate constants were obtained from first-order kinetic fits

		$10^{-6}\,k_{obs}/s^{-1}$				
Complex	λ/nm[b]	Ground state recovery	Excited state depletion	$(OC)_5W\cdots$solv growth	Excited state τ/ns	τ_{em}[c]/ns
1	355	5.3[d]	5.9[d]	4.7	170[d]	125
1	460	6.3[d]	7.1[d]	*e*	140[d]	
2 with excess 4,4'-bipy	355	5.6	4.2[d]	4.7[d]	240[d]	260
2	355	*f*	5.3	7.7	190	
2	420	5.9	4.5	*f*	220	
3	532				< 105[g]	

[a] All rates and lifetimes contain errors of approximately ± 10%. [b] Excitation wavelength. [c] Emission lifetimes recorded using 308 nm excitation. See ref. 12 for experimental details. [d] Average value, obtained either by duplicate experiments and/or averaging the data for one or more ν(CO) bands. [e] No $(OC)_5W\cdots$solv formed. [f] Traces too noisy to obtain accurate kinetic fit. [g] This lifetime approaches the detector response time and may therefore be inaccurate.

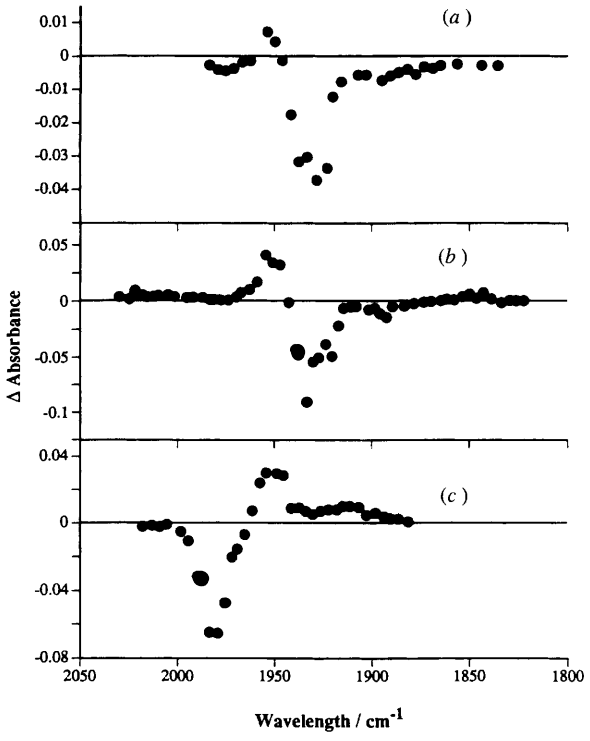

Fig. 5 (*a*) TRIR spectrum at 1 μs after the flash (355 nm, ≈30 mJ) of $[(OC)_5W(4,4'\text{-bipy})W(CO)_5]$ in CH_2Cl_2 solution (≈2.5 × 10^{-4} mol dm^{-3}, path length 2 mm);(*b*) TRIR spectrum at 1 μs after the flash (355 nm) of $[(OC)_5W(4,4'\text{-bipy})]$ in CH_2Cl_2 solution (1 ≈ × 10^{-3} mol dm^{-3}, path length 1 mm);(*c*) TRIR spectrum at 1 μs after the flash (355 nm) of $W(CO)_6$ in CH_2Cl_2 solution (path length 1 mm). Note in (*a*), the baseline is below the zero line; this is due to a small acoustic 'shock' wave which occurred at all frequencies during this experiment

$[(Pr^i_3P)_2(OC)_3Mo(pyz)]^+$. Similarly the cation of $[(R)\{(OC)_2Cr\}_2(\mu\text{-dppm})]$(dppm = $Ph_2PCH_2PPh_2$, R = biphenyl) shows a ν(CO) pattern[18] consistent with delocalisation with upward shifts in frequencies 'significantly less than those for the cation of the monomer $[(R)Cr(CO)_2(dppm)]$'. A rather similar argument applies to $[(H_3N)_5Ru(NC\text{–}CN)Ru(NH_3)_5]^{5+}$; a single ν(CN) band is observed in the IR at 2210 cm^{-1}, whereas the 4+ and 6+ cations show[19] ν(CN) bands at 1960 and 2330 cm^{-1} respectively.

In the localised case, two overlapping ν(CO) patterns are expected; one derived from the $(OC)_5W^{(\approx+1)}$ portion of the molecule, the other from the $W^{(\approx0)}(CO)_5$ group. The pattern of the bands associated with $(OC)_5W^{(\approx+1)}$ should be similar to that seen for the excited state of $[(OC)_5W(4,4'\text{-bipy})]$ and with similar shifts from the ground state. The bands for the neutral portion of the molecule, $W^{(\approx0)}(CO)_5$, should resemble the ground-state pattern, but with the bands displaced to somewhat *lower* frequency; back donation from the 4,4'-$bipy^-$ to the W^0, which in turn donates some electron density to the π* CO orbitals, would result in a downward shift in ν(CO) frequencies.

It is clear from Fig. 3(*a*) that the excited-state spectrum of **1** shows two overlapping ν(CO) patterns, one associated with $(OC)_5W^{(\approx+1)}$, the other with $W^{(\approx0)}(CO)_5$, and hence demonstrates a *localised* electron distribution.

We now turn to the low-frequency regions of the ν(CO) spectrum and see if the behaviour here is consistent with the model proposed above. However a complication arises with 355 nm irradiation. We saw that, on photolysis of **2** with 355 nm radiation, there is some production of $(OC)_5W\cdots$solv; in the high-frequency region this is easily resolved from the other band but the lower frequency region presents a problem. This is illustrated in Fig. 5, which shows TRIR experiments, recorded after 1 μs, on **1** and **2**, [Figs. 5(*a*) and 5(*b*) respectively] using a photolysis wavelength of 355 nm. The behaviour of $W(CO)_6$ under the same conditions is shown for comparison [Fig. 5(*c*)]. The TRIR spectra from **1** and **2** show loss of parent, and the generation of one band at 1954 cm^{-1}, which can be assigned to the e mode of $W(CO)_5\cdots$solv; note the low yield of $(OC)_5W\cdots$solv from **1**, consistent with the inability to detect the weaker high-frequency a_1 band described above. Fig. 5(*c*) shows loss of $W(CO)_6$ and the generation of two new bands at 1954 and 1912 cm^{-1}, corresponding to the e and low-frequency a_1 modes of $W(CO)_5\cdots$solv. Note that the low-frequency a_1 mode of $W(CO)_5\cdots$solv is obscured by parent depletion in the TRIR spectra of **1** and **2**.

In the case of **1**, the MLCT state is lower in energy than the LF state (Fig. 1). Thus, the use of a longer photolysis wavelength, at a lower energy than the dissociative LF state, should inhibit the production of $W(CO)_5\cdots$solv. Similar arguments apply to **2**, although it is suggested that the two levels are close together in **2**. The UV/VIS absorption spectra of **1** and **2**, and the wavelengths of the excitation sources are shown in Fig. 6.

The TRIR spectra at different times, following photolysis of **1** and **2** at 460 and 420 nm respectively, are shown in Fig. 7. After 100 ns both **1** and **2** show parent depletion and the generation of new spectral features to high frequency of the parent, and, in the case of **1**, clear indication of spectral features to low frequency of the parent absorptions. With **1**, as time lapses, there is loss of product bands and recovery of parent, which is complete by 1 μs. Thus with 460 nm photolysis there is no production of $(OC)_5W\cdots$solv. On the other hand with **2**,

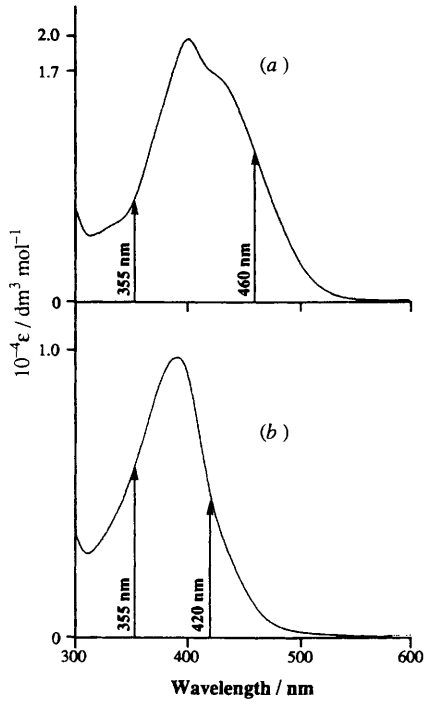

Fig. 6 UV/VIS absorption spectra in CH_2Cl_2 solution of (*a*) $[(OC)_5W(4,4'\text{-bipy})W(CO)_5]$ and (*b*) $[(OC)_5W(4,4'\text{-bipy})]$. The various photolysis wavelengths employed in the TRIR experiments are marked by arrows

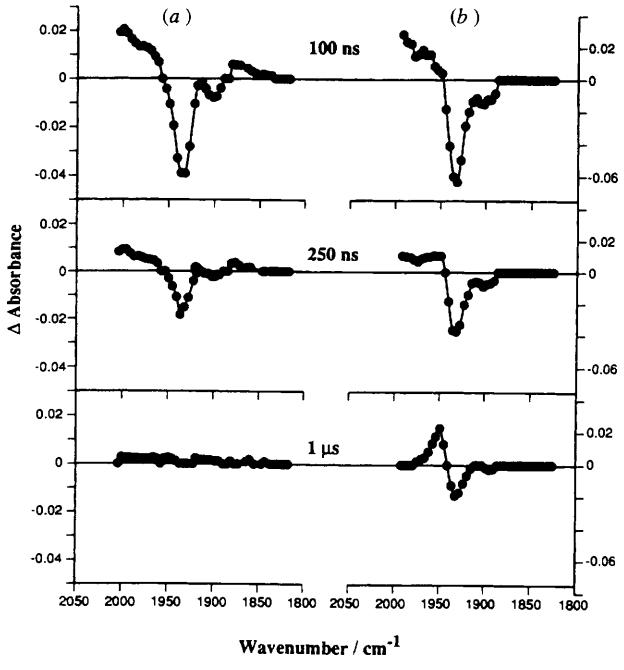

Fig. 7 (*a*) TRIR spectra recorded at 100 ns, 250 ns and 1 μs after flash (460 nm, ≈ 10 mJ) of $[(OC)_5W(4,4'\text{-bipy})W(CO)_5]$ in CH_2Cl_2 solution (≈ 5 × 10^{-4} mol dm^{-3}, path length 1 mm); (*b*) TRIR spectra recorded at 100 ns, 250 ns and 1 μs after flash (420 nm, ≈ 10 mJ) of $[(OC)_5W(4,4'\text{-bipy})]$ in CH_2Cl_2 solution (≈ 5 × 10^{-4} mol dm^{-3}, path length 1 mm)

at 1 μs there is incomplete recovery of parent and generation of $(OC)_5W \cdots$solv, identified by the e mode ν(CO) band at 1954 cm^{-1}. Note, however, that there is no evidence for 'instantaneous' production of $(OC)_5W \cdots$solv at 100 ns. These results are consistent with previous studies which showed a substantial decrease in the photodissociation quantum yield for **1** with increase in photolysis wavelength, whereas the

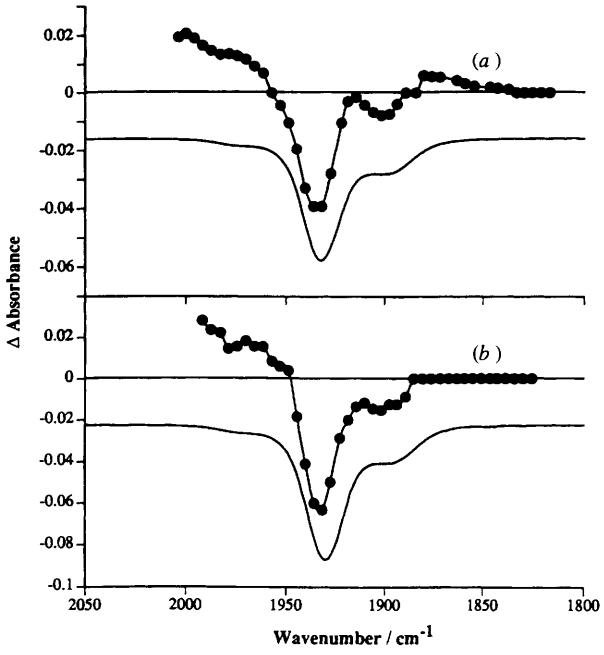

Fig. 8 TRIR spectrum at 100 ns after flash (460 nm, ≈ 10 mJ) of $[(OC)_5W(4,4'\text{-bipy})W(CO)_5]$ in CH_2Cl_2 solution (≈ 5 × 10^{-4} mol dm^{-3}, path length 1 mm); (*b*) TRIR spectrum at 100 ns after flash (420 nm, ≈ 10 mJ) of $[(OC)_5W(4,4'\text{-bipy})]$ in CH_2Cl_2 solution (≈ 5 × 10^{-4} mol dm^{-3}, path length 1 mm). Continuous lines displaced below the TRIR spectra represent the inverse of the ground-state FTIR spectra of the starting solutions

quantum yield for **2** remained significantly large at long wavelength.[3]

These results can be understood from Fig. 1. For **2**, 355 nm photolysis leads directly to the LF state and photodissociation; photolysis at 420 nm populates the MLCT state, which is sufficiently close to the LF state for the equilibrium between them to result in significant dissociation *via* the LF state. Similar results have been obtained in TRIR studies on the dissociation of $[(OC)_5W(L')]$ (L' = 4-cyano-[20] or 4-acetylpyridine[21]). On the other hand, for **1**, although 355 nm again leads to dissociation *via* the LF state, photolysis at 460 nm populates the MLCT state which, in this case, is too far away from the dissociative LF state for any equilibrium between them to be significant for dissociation.

We now look more closely at the photophysical behaviour. Fig. 8 shows the TRIR spectra of **1** and **2** recorded after 100 ns, employing 460 and 420 nm excitation wavelengths respectively. The continuous lines displaced below the TRIR spectra are the ground-state FTIR spectra, drawn with the absorption maxima pointing downwards. Fig. 8(*b*) shows depletion of **2** (1933, 1890 cm^{-1}) and the generation of one new band (1965 cm^{-1}) plus the low-frequency side of a second band to higher frequency. The peak of this second band falls outside the CO laser region, but its position (≈2005 cm^{-1}) has been obtained using the diode laser in conjunction with 355 nm photolysis. These two bands are readily assigned as the e and low-frequency a_1 ν(CO) bands of the carbonyl group in $(OC)_5W^+(4,4'\text{-bipy}^-)$ (Table 1). The similarity between the TRIR parent depletion profile and the FTIR band profile suggests that there are no product bands coincident with the parent absorptions or to low frequency of them.

Fig. 8(*a*) shows parent loss of **1** (1936, 1900 cm^{-1}) and several new features. To higher frequency of the parent appear two new broad bands (≈2010, ≈1970 cm^{-1}); these correspond to bands observed for the monomer and are similarly assigned to the $(CO)_5$ group attached to the oxidised W atom. There is clearly a new band at ≈1870 cm^{-1}, but this whole region is complicated

Table 3 Infrared vibrational data, in the ν(CO) region (in cm^{-1}), for the ground state, excited state and reduced complex for $[(OC)_5W(4,4'\text{-bipy})W(CO)_5]$ **1** and $[(OC)_5W(pyz)W(CO)_5]$ **3**

	Ground state[a]	Excited state[a,b]		Electrochemistry[c]		
Complex	FTIR	TRIR	Δ ν(CO)	Neutral	Anion	Δ ν(CO)
1	2072 (a_1)	2059	−13	2073	2064	−9
	1933 (e)	~1915	−18	1934	1922	−12
	1901 (a_1)	~1875	−26	1892	1871	−21
3	2069 (a_1)	2046	−23	2077	2057	−20
	1942 (e)	~1918	−24	1938	1918	−20
	1911 (a_1)	~1872	−39	1898	1852	−46

[a] Measured in CH_2Cl_2 solution (≈5 × 10^{-4} mol dm^{-3}). [b] Only the excited state bands decreasing in frequency are shown. [c] Measured in MeCN solution (≈5 × 10^{-4} mol dm^{-3}).

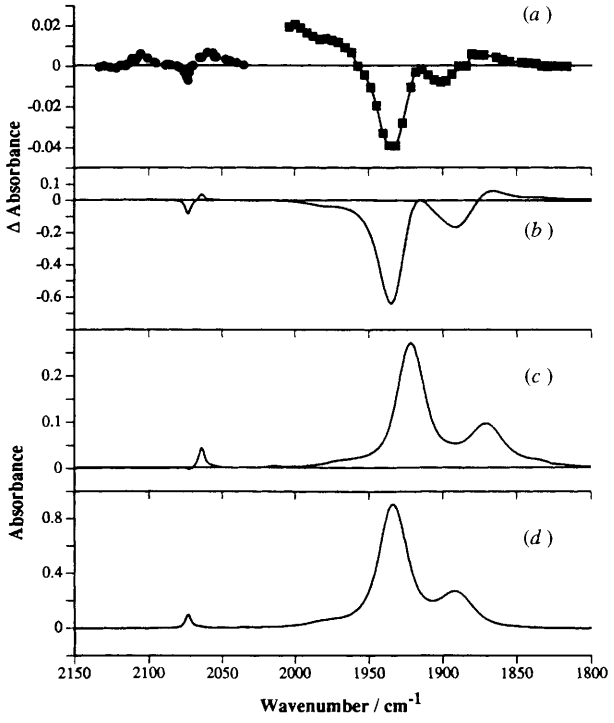

Fig. 9 TRIR spectra of $[(OC)_5W(4,4'\text{-bipy})W(CO)_5]$, recorded for ● at ≈85 ns after the flash (355 nm, 40 mJ) in CH_2Cl_2 solution (≈3.5 × 10^{-3} mol dm^{-3}, path length 1 mm) and for ■ at ≈100 ns after the flash (460 nm, ≈10 mJ) in CH_2Cl_2 solution (≈5 × 10^{-4} mol dm^{-3}, path length 1 mm). (*b*) and (*c*) FTIR subtraction spectra following relatively low electrochemical conversion of $[(OC)_5W(4,4'\text{-bipy})W(CO)_5]$ in MeCN solution (2 × 10^{-4} mol dm^{-3}, electrolyte NBu_4PF_6 ≈0.1 mol dm^{-3}, pathlength 2 mm) to $[(OC)_5W(4,4'\text{-bipy})W(CO)_5]^-$ with (*b*) the parent partially subtracted out and (*c*) the parent completely subtracted out. (*d*) FTIR spectrum of $[(OC)_5W(4,4'\text{-bipy})W(CO)_5]$ in MeCN solution (2 × 10^{-4} mol dm^{-3}, electrolyte NBu_4PF_6 ≈0.1 mol dm^{-3}, path length 2 mm)

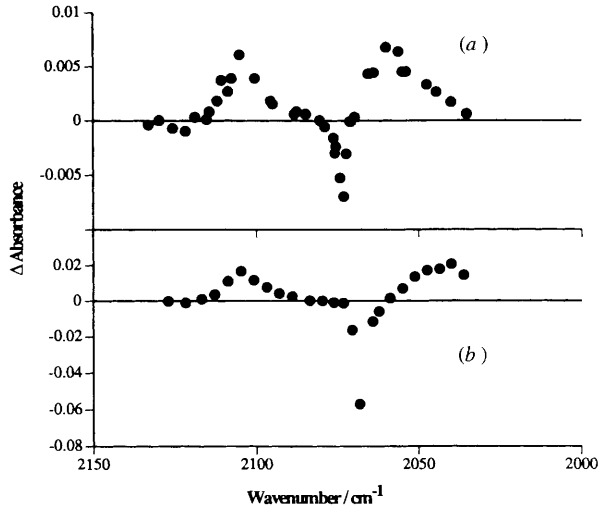

Fig. 10 (*a*) TRIR spectrum at ≈85 ns after flash (355 nm, ≈40 mJ) of $[(OC)_5W(4,4'\text{-bipy})W(CO)_5]$ in CH_2Cl_2 (≈3.5 × 10^{-3} mol dm^{-3}, path length 1 mm); (*b*) TRIR spectrum at ≈85 ns after flash (355 nm, ≈30 mJ) of $[(OC)_5W(pyz)W(CO)_5]$ in CH_2Cl_2 (≈5 × 10^{-4} mol dm^{-3}, path length 2.5 mm)

by overlap with the parent bands. However, there is evidence for a second band at ≈1915 cm^{-1}. This is seen more clearly in spectroelectrochemical experiments

Electrochemistry of $[(OC)_5W(4,4'\text{-bipy})W(CO)_5]$ **1**.—Monomer **2** has no reversible redox processes, hence its electrochemistry will not be considered further. The dimer **1** has two reversible one-electron reductions,[3] the first stage giving $\mathbf{1}^-$, $(OC)_5W(4,4'\text{-bipy}^-)W(CO)_5$. Thus the ν(CO) spectrum of $\mathbf{1}^-$ should give an indication of the effect of the 4,4′-$bipy^-$ group on those ν(CO) bands of **1*** assigned to the non-oxidised W. Spectroelectrochemical experiments on **1** in MeCN are summarised in Fig. 9; the TRIR spectra of the excited state of **1** in CH_2Cl_2 are included for comparison. Since any ν(CO) bands due to the doubly reduced species $\mathbf{1}^{2-}$ would complicate the spectrum, Fig. 9(*b*) shows a partial subtraction spectrum at relatively low conversion of **1** to $\mathbf{1}^-$. Ignoring the bands shifting to higher wavenumber in the excited state (2105, ≈2010 and ≈1970 cm^{-1}), comparison of the spectra of $\mathbf{1}^-$ and **1*** is very striking. The frequencies are given in Table 3. The spectrum of $\mathbf{1}^-$ can be easily obtained by complete subtraction of the parent bands shown in MeCN solution in Fig. 9(*d*), to give Fig. 9(*c*). The occurrence of only three ν(CO) bands in the spectrum of $\mathbf{1}^-$ is consistent with the two $W(CO)_5$ units being identical, as expected for $(OC)_5W(4,4'\text{-bipy}^-)W(CO)_5$. Unfortunately, the oxidation processes in both monomeric and dimeric molecules are irreversible;[3] however these oxidation processes in **5** and related species are reversible, and this has been taken advantage of by Kaim and co-workers[17] in spectroelectrochemical experiments.

TRIR and Electrochemistry of $[(OC)_5W(pyz)W(CO)_5]$ **3**.—As stated above, the excited state of $[(OC)_5W(pyz)]$ **4** is too short-lived to be studied on our present apparatus; thus we cannot interpret the excited-state IR spectrum of **3** by reference to that of the excited state of **4**. However the behaviour of **3** is very similar to that of **1**, and hence the interpretation is straightforward. Fig. 10(*b*) shows the high-frequency region of the TRIR spectrum of **3** following 532 nm excitation; it is possible to use excitation at this wavelength because the MLCT

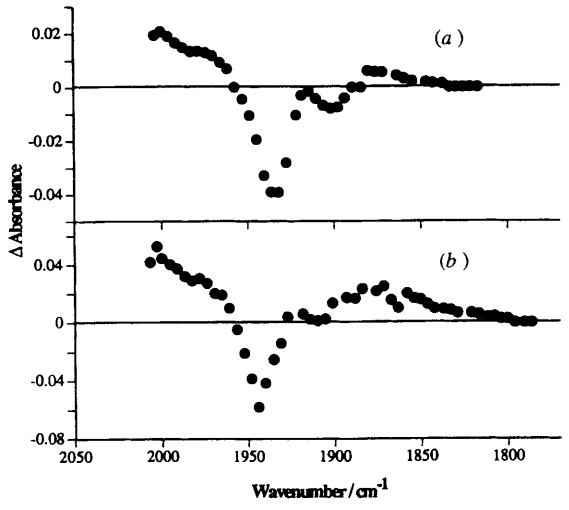

Fig. 11 (*a*) TRIR spectrum ≈100 ns after flash (460 nm, ≈10 mJ) of $[(OC)_5W(4,4'\text{-bipy})W(CO)_5]$ in CH_2Cl_2 solution (≈5 × 10^{-4} mol dm^{-3}, path length 1 mm); (*b*) TRIR spectrum ≈100 ns after flash (510 nm, ≈10 mJ) of $[(OC)_5W(pyz)W(CO)_5]$ in CH_2Cl_2 solution (≈5 × 10^{-4} mol dm^{-3}, path length 1 mm)

band of **3** has a maximum at 521 nm. Fig. 10(*a*) shows this spectral region of **1** and **1*** for comparison. Depletion of parent (2068 cm^{-1}) and the generation of two new bands (2105, ≈2046 cm^{-1}) are clearly visible [Fig. 10(*b*)]. The pattern of bands is the same as that seen for **1** [Fig. 10(*a*)], implying that the electron distribution in the excited state may be represented as $(OC)_5W^{(\approx+1)}pyz^{(\approx-1)}W^{(\approx0)}(CO)_5$. There was no evidence for dissociation to give $W(CO)_5 \cdots$ solv, and recovery of the parent was complete at 1 μs. Both excited state bands decayed with a lifetime of 105 ns (Table 2). As with **1**, this was shorter than previously measured by emission (186 ns in benzene solution[3]), the difference again being due to solvent change. It should be noted that this lifetime value approaches the response time of the detector and therefore the value of 105 ns represents an upper limit.

The TRIR studies on **3** in the low ν(CO) region are shown in Fig. 11, again with **1** for comparison. The spectra of **1** [Fig. 11(*a*)] and **3** [Fig. 11(*b*)] show similar key features: two bands moving to higher frequency (2003, 1978 cm^{-1}) for **3**, a band shifting to lower frequency of the parent (≈1872 cm^{-1}), and the distortion of the parent depletion profile caused by the overlap with an excited state band (≈1918 cm^{-1}).

Electrochemical experiments on **3**, not so well defined as for **1**, are summarised in Fig. 12; the TRIR spectra are included for comparison [Fig. 12(*a*)]. Fig. 12(*b*) shows a partial subtraction spectrum at relatively low conversion of **3** to $\mathbf{3}^-$, and Fig. 12(*c*) shows the spectrum with all the parent subtracted. The electrochemical and corresponding TRIR data for **3** are given in Table 3.

The behaviour of **3** in electrochemical experiments was again similar to that of **1**, where, following one-electron reduction, the three ground-state absorptions (2077, 1938 and 1898 cm^{-1}) of **1** shifted to lower frequency (2057, 1918 and 1852 cm^{-1}). The similarity between the band positions for $\mathbf{3}^-$ and those shifting downwards in **3***, again strongly support an excited-state structure of $(OC)_5W^{(\approx+1)}pyz^{(\approx-1)}W^{(\approx0)}(CO)_5$.

Localisation/Delocalisation.—There is great interest in the question of localisation *versus* delocalisation in mixed-valence compounds. Of course the definition really depends on the spectroscopic technique being used to probe the behaviour. Because of the relationships, $\Delta E \times \Delta t \geq h/2\pi$, and $\Delta E = h\Delta\nu$, coalescing of two spectral features, and hence 'delocalisation', will occur if $\Delta t < 1/2\pi\Delta\nu$, *i.e.* $k > 2\pi\Delta\nu$.

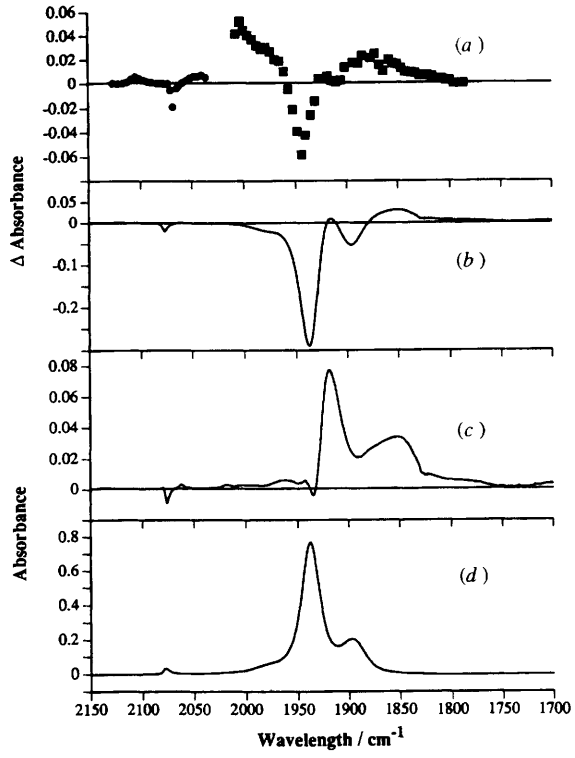

Fig. 12 TRIR spectra of $[(OC)_5W(pyz)W(CO)_5]$, recorded for ● at ≈85 ns after the flash (532 nm, ≈30 mJ) in CH_2Cl_2 solution (≈5 × 10^{-4} mol dm^{-3}, path length 2.5 mm) and for ■ at ≈100 ns after the flash (510 nm, ≈10 mJ) in CH_2Cl_2 solution (≈5 × 10^{-4} mol dm^{-3}, path length 1 mm). (*b*) and (*c*) FTIR subtraction spectra following relatively low electrochemical conversion of $[(OC)_5W(pyz)W(CO)_5]$ in MeCN solution (≈4 × 10^{-4} mol dm^{-3}, electrolyte NBu_4PF_6 ≈0.1 mol dm^{-3}, path length 2 mm) to $[(OC)_5W(pyz)W(CO)_5]^-$ with (*b*) the parent partially subtracted out and (*c*) the parent completely subtracted out. (*d*) FTIR spectrum of $[(OC)_5W(pyz)W(CO)_5]$ in MeCN solution (≈4 × 10^{-4} mol dm^{-3}, electrolyte NBu_4PF_6 ≈0.1 mol dm^{-3}, path length 2 mm). Note the TRIR spectra denoted by ● has been scaled by a factor of three to allow for changes in path length

The two high-frequency a_1 ν(CO) bands of the excited states of **1** and **3**, do not coalesce and are separated by (≈2105 − 2059) ≈46 cm^{-1}, and (≈2105 − 2046) ≈59 cm^{-1}, respectively. Therefore the rate of electron exchange in **1*** and **3*** must be ≪9 × 10^{12} s^{-1} and ≪1.1 × 10^{13} s^{-1} respectively.

There have been other relevant spectroscopic studies on excited states. The excited state of $[(NC)(2,2'\text{-bipy})_2Ru^{II}(CN)\text{-}Ru^{II}(2,2'\text{-bipy})_2(CN)]^+$ (2,2'-bipy = 2,2'-bipyridyl) shows *two* terminal CN stretches in the TRIR spectrum at 2090 and 2106 cm^{-1}, compared with a *single* band at 2079 cm^{-1} in the ground state.[22] This is a clear indication of a localised excited state, $[(NC)(2,2'\text{-bipy})_2Ru^{II}(CN)Ru^{III}(2,2'\text{-bipy}^-)(2,2'\text{-bipy})\text{-}(CN)]^{+*}$, where, using the argument above the rate of electron exchange is ≪3 × 10^{12} s^{-1}. Similar conclusions, based on time-resolved resonance-Raman and absorption spectroscopy, have been obtained recently for related CN-bridged Ru species.[23] In these complexes the excited state involves electron transfer to a group in a terminal position, whereas for **1** and **3**, the excited state involves electron transfer to the bridging ligand. Meyer and co-workers[24] have examined the excited-state properties of a number of species with a 4,4'-bipyridyl bridging group. The excited state of $[(2,2'\text{-bipy})(CO)_3Re^{I}(4,4'\text{-bipy})\text{-}Re^{I}(CO)_3(2,2'\text{-bipy})]^{2+}$ can involve either electron transfer to the terminal 2,2'-bipy or the bridging 4,4'-bipy, depending on the solvent, and these two states are in rapid equilibrium.[24] There is unfortunately no evidence as to whether either of the two excited states is localised or delocalised. The Re system

can be 'tuned' by substituting on the terminal bipy groups,[25] *i.e.* $[(4,4'\text{-}X_2\text{-}2,2'\text{-bipy})(CO)_3Re^I(\mu\text{-}4,4'\text{-bipy})Re^I(CO)_3(4,4'\text{-}Y_2\text{-}2,2'\text{-bipy})]^{2+}$ which, depending on the nature of X and Y, have the lowest excited MLCT state on either the bridging or terminal ligands; again there is no evidence about localisation/delocalisation, and such species would benefit from time-resolved vibrational studies.

Class I/Class II Behaviour.—In the above discussion it has been tacitly assumed that the complexes in the excited state display mixed-valence Class II.[11] The argument that the excited states are localised can also apply to Class I mixed-valence species. The distinction between Class I and Class II depends on evidence for coupling (in the usual notation $2H_{AB}$) between the two halves of the molecule; $2H_{AB} \approx 0$ for Class I, and $2H_{AB} > 0$ for Class II. In principle the inter-valence transition (*e.g.* for the excited state of **1**, schematically $W^+L^-W \longrightarrow WL^-W^+$) provides direct evidence for the degree of coupling. So far, for none of these species has evidence for an inter-valence transition been obtained. In the absence of this evidence we have to look in more detail at the vibrational data.

Consider the general system (ALA) with a charge-transfer excited state (A^+L^-A). We compare the spectral properties of the two units of the excited state $[A^+L^-]$ and $[L^-A]$, respectively with those of the excited state (A^+L^-) and anion (L^-A) of the monomer (AL). For Class I and Class II behaviour the spectral properties will be, respectively, similar and different.

It is clear from Table 1 that shifts to high frequency in the excited state of **1** are almost identical to those for **2**. This presents half the evidence for Class I. Unfortunately, because of decomposition, it is not possible to examine the IR spectroelectrochemistry of **2**, and we have to compare the excited state spectrum of **1** with the spectrum of $\mathbf{1}^-$. This presents a problem since we might expect the ν(CO) spectrum of $\mathbf{1}^-$ compared with **1** to show shifts considerably less than those of $\mathbf{2}^-$ compared with **2**. This is turn means that Class I behaviour requires that the low-frequency ν(CO) shifts for $\mathbf{1}^-$ from **1** be less than those of **1*** from **1**. Table 3 in fact shows precisely this behaviour, which is thus consistent with Class I behaviour for **1**. Surprisingly the low-frequency ν(CO) shifts **3** to **3*** are very similar to **3** to $\mathbf{3}^-$, but it must be noted that the electrochemical data for $\mathbf{3}^-$ are not very accurate. It is also worth noting that although the upward shifts for **1** and **3** are approximately equal (Table 1), indicating a similar degree of oxidation of one of the W atoms, the downward shifts are much greater for **3** than for **1**. This can be explained by the less extensive π system for pyrazine, compared with 4,4'-bipy, resulting in 'greater charge leakage' to the formally neutral W atom in the excited state. A similar effect is observed in the electrochemical experiments where the downward ν(CO) shift for $\mathbf{3} \longrightarrow \mathbf{3}^-$ is greater than for $\mathbf{1} \longrightarrow \mathbf{1}^-$.

Conclusion

The electron distributions in the lowest excited states of **1**, **2** and **3** have been unambiguously determined from ν(CO) IR data; **1*** and **3*** clearly show localised behaviour on the IR 'time-scale', their structures being summarised as $(OC)_5W^{(\approx +1)}L^{(\approx -1)}\text{-}W^{(\approx 0)}(CO)_5$ (where L = 4,4'-bipy or pyz). The spectral data also suggest that the excited states display behaviour more characteristic of Class I than Class II. Thus, the importance of TRIR as a probe for electron transfer has been demonstrated once more. The importance of the complementary technique of spectroelectrochemistry has also been illustrated, the single-electron reduction data for **1** and **3** proving to be a good model for the neutral portion of the excited state, $L^{(\approx -1)}W^{(\approx 0)}(CO)_5$.

Acknowledgments

We thank the SERC (GR/H63296), EC Human Capital and Mobility, Mütek GmbH and Perkin-Elmer for support. We have had many helpful discussions with Professor A. J. Lees, Drs. J. J. McGarvey, E. S. Dodsworth and A. Vlcek, jun.

References

1 S. Chun, D. C. Palmer, E. F. Mattimore and A. J. Lees, *Inorg. Chim. Acta*, 1983, **77**, L119.
2 A. J. Lees, J. M. Fobare and E. F. Mattimore, *Inorg. Chem.*, 1984, **23**, 2709.
3 M. M. Zulu and A. J. Lees, *Inorg. Chem.*, 1988, **27**, 1139.
4 M. M. Zulu and A. J. Lees, *Inorg. Chem.*, 1989, **28**, 85.
5 W. Kaim and S. Kohlmann, *Inorg. Chem.*, 1990, **29**, 1898.
6 E. S. Dodsworth and A. B. P. Lever, *Inorg. Chem.*, 1990, **29**, 499.
7 P. L. Gaus, J. M. Boncella, K. S. Rosengren and M. O. Funk, *Inorg. Chem.*, 1982, **21**, 2174.
8 R. J. Crutchley, *Adv. Inorg. Chem.*, 1994, **41**, 273.
9 R-A. McNicholl, J. J. McGarvey, A. H. R. Al-Obaidi, S. E. J. Bell, P. M. Jayaweera and C. G. Coates, *J. Phys. Chem.*, in the press.
10 M. W. George, J. J. Turner and J. R. Westwell, *J. Chem. Soc., Dalton Trans.*, 1994, 2217.
11 M. B. Robin and P. Day, *Adv. Inorg. Chem. Radiochem.*, 1967, **10**, 247.
12 J. R. Westwell, Ph.D. Thesis, University of Nottingham, 1994.
13 M. W. George, M Poliakoff and J. J. Turner, *Analyst*, 1994, **119**, 551.
14 O. Ishitani, M. W. George, T. Ibusuki, F. P. A. Johnson, K. Koike, K. Nozaki, C. Pac, J. J. Turner and J. R. Westwell, *Inorg. Chem.*, 1994, **33**, 4712; M. Oyama, K. Nozaki, H. Hatano and S. Okazaki, *Bull. Chem. Soc. Jpn.*, 1989, **93**, 8304.
15 F. P. A. Johnson, M. W. George, S. L. Morrison and J. J. Turner, *J. Chem. Soc., Chem. Commun.*, 1995, 391.
16 P. M. Hodges, S. A. Jackson, J. Jacke, M. Poliakoff, J. J. Turner and F-W. Grevels, *J. Am. Chem. Soc.*, 1990, **112**, 1234.
17 W. Bruns, W. Kaim, E. Waldhor and M. Krejçik, *J. Chem. Soc., Chem. Commun.*, 1993, 1868.
18 N. van Order, jun., W. E. Geiger, T. E. Bitterwolf and A. L. Rheingold, *J. Am. Chem. Soc.*, 1987, **109**, 5680.
19 H. Taube, *Ann. N. Y. Acad. Sci.*, 1978, **313**, 481; G. M. Thom and H. Taube, *J. Am. Chem. Soc.*, 1975, **97**, 5310; see also C. Kreutz, *Prog. Inorg. Chem.*, 1983, **30**, 1.
20 P. Glyn, F. P. A. Johnson, M. W. George, A. J. Lees and J. J. Turner, *Inorg. Chem.*, 1991, **30**, 3543.
21 F. P. A. Johnson, M. W. George and J. J. Turner, *Inorg. Chem.*, 1993, **32**, 4226.
22 C. A. Bignozzi, R. Argazzi, J. R. Schoonover, K. C. Gordon, R. B. Dyer and F. Scandola, *Inorg. Chem.*, 1992, **31**, 5260.
23 C. A. Bignozzi, C. Chiorboli, F. Scandola, R. B. Dyer, J. R. Schoonover and T. J. Meyer, *Inorg. Chem.*, 1994, **33**, 1652.
24 G. Tapolsky, R. Duesing and T. J. Meyer, *J. Phys. Chem.*, 1991, **95**, 1105.
25 G. Tapolsky, R. Duesing and T. J. Meyer, *Inorg. Chem.*, 1990, **29**, 2285.

Received 15*th March* 1995; *Paper* 5/01644D